Journal of Analytical Science and Technology

RESEARCH ARTICLE Open Access

A short novel antimicrobial peptide BP100-W with antimicrobial, antibiofilm and anti-inflammatory activities designed by replacement with tryptophan

Chelladurai Ajish[1†], S. Dinesh Kumar[1†], Eun Young Kim[1], Sungtae Yang[2] and Song Yub Shin[1*]

Abstract

BP100 is a short cationic antimicrobial peptide (AMP) designed using a combinatorial chemistry approach based on the cecropin A-melittin hybrid. It displays potent antimicrobial activity against gram-negative bacteria and low toxicity toward eukaryotic cells. To develop a short AMP with potent cell selectivity, antibiofilm and anti-inflammatory activities, we designed a newly BP100 analog, BP100-W, in which Leu-3 at the hydrophobic face of BP100 was replaced by Trp. BP100-W possessed better cell selectivity, with a 1.7-fold higher therapeutic index than BP100. BP100-W displayed more effective synergistic activity when combined with several antibiotics, such as chloramphenicol, ciprofloxacin and oxacillin, compared to BP-100. BP100-W also exhibited stronger antibiofilm activity than BP100 in inhibiting biofilm formation by multidrug-resistant *Pseudomonas aeruginosa* (MDRPA) and eradicating the preformed biofilms of MDRPA. Moreover, unlike BP100, BP100-W significantly suppressed the production and expression of lipopolysaccharide (LPS)-induced pro-inflammatory cytokines, such as the tumor necrosis factor-α and nitric oxide. Boron-dipyrromethene-TR-cadaverine displacement assay demonstrated that the inhibitory activity of BP100-W on LPS-induced inflammation in RAW 264.7 cells may be due to increased direct interaction with LPS. Our results suggest that BP100-W exhibits potential for future use as an antimicrobial, antibiofilm and anti-inflammatory agent.

Keywords: Antimicrobial peptide, Cell selectivity, Antibiofilm activity, Anti-inflammatory activity, Synergistic activity

Introduction

BP100 is a short cationic antimicrobial peptide (AMP) of 11 amino acid residues (KKLFKKILKYL-NH_2) designed by the combinatorial chemistry of a hybrid of cecropin A (an AMP from the moth *Hyalophora cecropia*) and melittin (an AMP from bee venom) (Badosa et al. 2007). This peptide displayed potent antimicrobial activity against gram-negative bacteria, low toxicity toward eukaryotic dells, efficient cell-penetrating ability and low susceptibility to proteinase K degradation (Ferre et al. 2009). BP100 acquires an α-helical conformation upon interaction with membranes and increases membrane permeability. The secondary structure formation and bacterial killing performance of BP100 appear to be directly related to the negative charge content of the membrane, thus explaining its high selectivity toward negative bacterial membranes and low cytotoxicity against predominantly less negatively charged mammalian cell membranes (Epand et al. 2007). Replacing lysine (Lys) and tyrosine (Tyr) in BP100 with arginine (Arg) and tryptophan (Trp), respectively, significantly increases the antimicrobial activity against gram-positive bacteria (Torcato et al. 2013). The amphipathic property of AMPs and the balance between electrostatic and hydrophobic

†Chelladurai Ajish and S. Dinesh Kumar contributed equally to this work.

*Correspondence: syshin@chosun.ac.kr

[1] Department of Cellular and Molecular Medicine, School of Medicine, Chosun University, Gwangju 61452, Republic of Korea
Full list of author information is available at the end of the article

interactions with bacterial membranes are determinant for their membrane-targeting activity, such as is the case of cecropin–melittin hybrid peptides (Bastos et al. 2008; Ferre et al. 2009; Juvvadi et al. 1996) or Trp-rich peptides (Arias et al. 2014; Mishra et al. 2018; Wei et al. 2006). Trp is stable at the interface of a hydrophilic extracellular environment and the hydrophobic interior of the bacterial membrane, allowing peptides to be firmly inserted into the bacterial membrane, thus causing membrane disruption (Bi et al. 2014; Killian and Heijne 2000; Yau et al. 1998). Trp-rich peptide indolicidin have been shown to bind various molecules like DNA (Ghosh et al. 2014; Hsu et al. 2005; Marchand et al. 2006), calmodulin (Sitaram et al. 2003) and ATP (Hilpert et al. 2010). Trp-rich peptide tritrpticin has been proposed to participate in ring-stacking interaction with nucleic acid bases (Sharma et al. 2013). However, how the multiple Trp residues of these Trp-rich peptides relate to their antimicrobial action is still unclear.

In this study, we synthesized a newly BP100 analog, BP100-W (KKWFKKILKYL-NH_2), in which Leu-3 at the hydrophobic face of BP100 was replaced by Trp and studied its biological activities, including antimicrobial, hemolytic, synergistic, antibiofilm and anti-inflammatory activities. Cell selectivity of the peptides was determined by examining their antimicrobial activity against gram-positive and gram-negative bacterial strains, and hemolytic activity against sheep red blood cells (sRBCs). A checkerboard titration experiment was performed to evaluate the synergistic activities of the peptides and different conventional antibiotics (ciprofloxacin, chloramphenicol and oxacillin) against multidrug-resistant *Pseudomonas aeruginosa* (MDRPA) and methicillin-resistant *Staphylococcus aureus* (MRSA). Antibiofilm activity of the peptides in inhibiting MDRPA biofilm formation and eradicating preformed MDRPA biofilms was assessed by measuring the minimum biofilm inhibitory concentration (MBIC) and minimum biofilm eradication concentration (MBEC), respectively. Furthermore, anti-inflammatory activity of the peptides was evaluated by investigating the suppression of nitric oxide (NO) and tumor necrosis factor (TNF)-α production and mRNA expression in lipopolysaccharide (LPS)-stimulated mouse macrophage RAW264.7 cells. Furthermore, to determine whether the anti-inflammatory activity of the peptide against LPS-stimulated inflammation is due to its direct-LPS binding, an LPS-binding assay was performed.

Materials and methods

Materials and bacteria strains

9-Fluorenylmethoxycarbonyl (Fmoc) protected amino acids and rink amide 4-methylbenzhydrylamine (MBHA) resin were purchased from Novabiochem (La Jolla, CA, USA). Chloramphenicol (CHL), ciprofloxacin (CIP) and oxacillin (OXA) were purchased from Sigma-Aldrich (St. Louis, MO, USA). *Escherichia coli* (KCTC 1682), *Pseudomonas aeruginosa* (KCTC 1637), *Salmonella typhimurium* (KCTC 1926), *Bacillus subtilis* (KCTC 3068), *Staphylococcus epidermidis* (KCTC 1917) and *Staphylococcus aureus* (KCTC 1621) were supplied from the Korean Collection for Type Cultures (KCTC) of the Korea Research Institute of Bioscience and Biotechnology (KRIBB). MDRPA (CCARM 2095) and MRSA (CCARM 3090) were obtained from the Culture Collection of Antibiotic-Resistant Microbes (CCARM) of Seoul Women's University, Republic of Korea. RAW264.7 (mouse macrophage) cells were procured from the American Type Culture Collection (Manassas, VA).

Peptide synthesis

The peptides (BP100 and BP100-W) were manually synthesized using Rink Amide MBHA resin and 9-fluoromethyloxycarbonyl (Fmoc)-based solid phase peptide synthesis (SPPS). The peptides were purified by reverse phase high-performance liquid chromatography (RP-HPLC) with a Vydac C18 column (250 × 25 mm, 5 µm pore size). The purity of the peptides was confirmed by analytical RP-HPLC with a Vydac C_{18} column (4.6 × 250 mm, 5 µm pore size). The masses of the peptides were confirmed by matrix-assisted laser desorption ionization-time-of-flight mass (MALDI-TOF MS) spectrometry (Shimadzu, Japan).

Circular dichroism (CD) analysis

Circular dichroism (CD) spectroscopy of the peptides (100 µg/ml) was detected in 10 mM phosphate-buffered saline (PBS), 50% trifluoroethanol (TFE) and 30 mM sodium dodecyl sulfate (SDS) on a JASCO-715 spectropolarimeter (Jasco, Japan) at room temperature, with a quartz cuvette with a 1-mm path length. The spectra were recorded from 190 to 250 nm at a scanning speed of 10 nm/min, and an average of 3 scans was collected for each peptide. Finally, the mean residue ellipticity was calculated as previously described method (Rajasekaran et al. 2019).

Antimicrobial activity

Minimum inhibitory concentration (MIC) of the peptides was determined using broth microdilution method (Kumar and Shin 2020; Wiegand et al. 2008). Briefly, mid-log phase cultures were diluted with Mueller–Hinton broth and added to sterile 96-well plates containing twofold serially diluted peptides (from 2 to 128 µM) in 1:1 ratio to give final cell concentration of 2×10^6 CFU/wells. Melittin treated cells were used as positive control while untreated cells were used as a negative control. The

minimal inhibitory concentration (MIC) was defined as the lowest peptide concentration that causes 100% inhibition of microbial growth after incubation at 37 °C for 24 h. All experiments were performed in duplicate in three independent experiments.

Hemolytic activity

The hemolytic activity of peptides was determined by measuring the amount of free hemoglobin by the lysis of erythrocytes using sRBCs as previously described (Dong et al. 2012). Fresh sRBCs were washed three times with 1 × PBS (pH 7.2) followed by centrifugation for 5 min at 116 × g. 4% (w/v) . sRBC suspension was added to PBS containing peptides (2–512 μM). After incubation for 1 h at 37 °C, the samples were centrifuged at 1000 × g for 5 min. Absorbance of supernatant (hemoglobin) was measured using a microplate enzyme-linked immunosorbent assay (ELISA) reader (Bio-Tek Instruments EL800, USA) at 540 nm. As a positive control, 100% hemolysis was induced by treating sRBCs with 0.1% Triton X-100. The value for "zero hemolysis" was determined using PBS. Three replicates were evaluated under each condition.

Cytotoxicity against RAW 264.7 cells

To determine the cytotoxicity of the peptides, we used the MTT [3-(4, 5-dimethylthiazol-2-yl)-2, 5-diphenyltetrazolium bromide] dye reduction assay against RAW 264.7 cells as previously described (Zhu et al. 2014). Briefly, the cells were seeded in 96-well plates (2×10^4 cells/well) and cultured for 24 h at 37 °C. Increasing concentrations of the peptides were added and allowed to react with the cells for 48 h, followed by the addition of 20 μl MTT (5 mg/ml in PBS) for another 4 h at 37 °C. The formazan produced was dissolved in dimethyl sulfoxide (DMSO), and the absorbance at 550 nm was measured using a microplate ELISA reader. A 100% cytotoxic control was generated by treatment with 0.1% Triton X-100. Three replicates were evaluated under each condition.

Checkerboard titration assay

The checkerboard titration assay is performed to evaluate the combinatorial effects of the peptides and conventional antibiotics as described elsewhere (Khara et al. 2014). Initially, twofold serial dilutions of the peptide and three antibiotics (chloramphenicol, oxacillin and ciprofloxacin) were prepared and added in 1:1 ratio to 96-well plate. An equal volume of bacterial solution (100 μL) at ~ 10^6 CFU/mL was added to each well. The plates were then incubated in a shaking incubator at 37 °C for 24 h. Bacterial growth was assessed spectrophotometrically at absorbance 600 nm using microplate ELISA reader (EL800, Bio-Tek instrument). The fractional inhibitory concentration (FIC) index (FICI) was calculated as follows: FICI = [(MIC of peptide in combination)/(MIC of peptide alone)] + [(MIC of antibiotic in combination)/(MIC of antibiotic alone)]. The fractional inhibitory concentration index (FICI) ≤ 0.5 is considered as indicative of synergy; 0.5 < FICI ≤ 1.0 is considered as additive; 1.0 < FICI ≤ 4.0 is considered as indifferent; and FICI > 4.0 is considered as indicative of antagonism.

Biofilm inhibition assay (MBIC)

Biofilm quantification was carried out as described elsewhere (Basak et al. 2017; Harrison et al. 2010). Briefly, 1×10^6 CFU/200 μl of MDRPA strain (CCARM 2095) in Mueller Hinton broth (MHB) with 0.2% glucose was incubated at 37 °C for 24 h in 96-well microtiter plates, with or without peptides. After the incubation, the planktonic bacteria were removed by washing three times with PBS solution. Afterward, 99% methanol was added and fixed for 15 min. After aspiration, the plates were allowed to dry. Dried wells were stained with 100 μl of 0.1% crystal violet for 5 min, and excess stain was gently rinsed off with tap water. Stain was resolubilized in 95% ethanol, and absorbance at 600 nm was measured. Untreated bacteria were used as the control. All biofilm inhibition assays were performed in triplicate. The concentration of the peptide that completely prevented residual CV staining/biomass was the MBIC.

Biofilm eradication assay (MBEC)

Minimal biofilm eradication concentration (MBEC) of the peptides against preformed MDRPA (CCARM 2095) biofilms was determined using Calgary Biofilm Device (Innovotech, Edmonton, Canada), as previously described (Basak et al. 2017; Harrison et al. 2010). Briefly, 1×10^6 CFU/mL of bacteria was suspended in 150 μL of appropriate nutrient media (LB media) and placed in 96-well microtiter plates with peg lids (Innovotech, Edmonton, Canada; product code: 19,111) to establish biofilms. Plates were sealed with parafilm and incubated at 37 °C for 24 h in a shaking incubator at 110 rpm. Lids of the plates were then removed, rinsed with 0.01 M PBS, and transferred to sterile 96-well plates containing serial dilutions of the compounds: the final volume with the media was 200 μL/well. Plates were then incubated at 37 °C for 24 h in a shaking incubator at 110 rpm. After 24 h of treatment, the peg lid of each plate was removed, rinsed with buffer, and transferred to a recovery plate containing 200 μL of nutrient media. Recovery plates were thereafter sonicated in a water bath for 10–15 min to dislodge biofilms. Peg lids were removed and plates were incubated overnight (for 24 h) at 37 °C in a shaking incubator at 110 rpm to recover viable bacteria, resulting in turbidity. The MBEC values were recorded as the

lowest concentration resulting in eradication of the biofilm (i.e., no turbidity after the final incubation period relative to sterility controls). Experiments were performed in triplicate, and the median value of each experiment was presented.

Production of nitric oxide (NO) from LPS-stimulated RAW264.7 cells

RAW264.7 cells were plated at a density of 5×10^5 cells/ml in 96-well culture plates and stimulated with LPS from *E. coli* O111:B4 (20 ng/mL) in the presence or absence of peptides for 24 h. Isolated supernatant fractions were mixed with an equal volume of Griess reagent (1% sulfanilamide, 0.1% naphthylethylenediamine dihydrochloride and 2% phosphoric acid) and incubated at room temperature for 10 min. Nitrite production was quantified by measuring absorbance at 540 nm, and concentrations were determined using a standard curve generated with $NaNO_2$.

TNF-α release from LPS-stimulated RAW264.7 cells

RAW264.7 cells were seeded in 96-well plates (5×10^4 cells/well) and incubated overnight. Peptides were added and the cultures were incubated at 37 °C for 1 h. Subsequently, LPS from *E. coli* O111:B4 (20 ng/mL) was added and the cells were incubated for another 6 h at 37 °C. The concentration of TNF-α in each sample was measured using a mouse TNF-α ELISA kit (R&D Systems, Minneapolis, MN, USA) according to the manufacturer's protocol.

Reverse-transcription polymerase chain reaction (RT-PCR)

RT-PCR assay for expression of LPS-induced iNOS and TNF-α was determined using semi-quantitative reverse-transcription PCR as previously described (Kumar and Shin 2020; Rajasekaran et al. 2019). Briefly, RAW264.7 cells were seeded into 6-well plates at 2×10^6 cells/well and stimulated with *E. coli* O111:B4 LPS (20 ng/mL) in the presence or absence of peptides. After incubation of 3 h (for TNF-α) and 6 h (for inducible nitric oxide synthase (iNOS)), total RNA was extracted using TRIzol® reagent (Invitrogen) and RNA concentration quantified using Nanodrop spectrophotometer (BioDrop, UK). cDNA was synthesized from 2 mg of total RNA using Oligo-d(T)15 primers and PrimeScript Reverse Transcriptase kit (Takara, Japan) according to the manufacturer's protocol. The cDNA products were amplified using following primers: iNOS (forward 50-CTGCAG CACTTGGATCAGGAACCTG-3′, reverse 5′-GGGAGT AGCCTGTGTGCACCTGGAA-3′); TNF-α (forward 5′- CCTGTAGCCCACGTCGTAGC-3′, reverse 5′-TTG ACCTCAGCGCTGAGTTG-3′) and GAPDH (forward 5′-GAGTCAACGGATTTGGTCGT-3′, reverse 5′- GAC AAGCTTCCCGTTCTCAG-3′). The PCR amplification was carried out for initial denaturation at 94 °C for 5 min, followed by forty cycles of denaturation at 94 °C for 1 min, annealing at 55 °C for 120 s and extension at 72 °C for 1 min, with a final extension at 72 °C for 5 min. The PCR products were separated by electrophoresis and visualized under UV illumination.

LPS-binding assay

The LPS-binding ability of the peptides was determined by a BODIPY-TRcadaverine (BC) displacement assay (Wood et al. 2004). Briefly, LPS from *E. coli* O111:B4 (25 μg/ml) was incubated with BC (2.5 μg/ml) and peptide (1-32 μM) in Tris buffer (50 mM, pH 7.4) for 4 h. A volume of 2 ml of this mixture was added to a quartz cuvette. Fluorescence was recorded at an excitation wavelength of 580 nm and an emission wavelength of 620 nm with a Shimadzu RF-5301 PC fluorescence spectrophotometer (Shimadzu Scientific Instruments). The percentage fluorescence was calculated using formula: $\%\Delta F\ (AU) = [(F_{obs} - F_0)/(F_{100} - F_0)] \times 100$, where Fobs is the observed fluorescence at a given peptide concentration, F_0 is the initial fluorescence of BC with LPS in the absence of peptides, and F_{100} is the BC fluorescence with LPS cells upon the addition of 10 μg/ml polymyxin B.

Results and discussions

Peptide design and synthesis

Amino acid sequences of BP100 and BP100-W generated in this study are summarized in Table 1. The α-helical wheel diagram of BP100 and BP100-W was predicted using the online analysis tool, HeliQuest server (https://heliquest.ipmc.cnrs.fr/cgi-bin/ComputParams.py) (Fig. 1). The results showed that BP100 and BP100-W carry a +5 net charge with hydrophobic moment of 0.847 and 0.873, respectively (Table 1). BP100 and BP100-W adopt an amphipathic α-helical structure because the hydrophobic and positively charged residues are spatially arranged opposite to each other (Fig. 1). Compared to other hydrophobic amino acid residues, such as Leu, Ile and Val, Trp residue is thought to facilitate the interface association between AMPs and the lipid bilayer and mediate the cohesive hydrophobic interactions with lipid acyl chains during membrane disruption. (Sanchez et al. 2011; Yau et al. 1998). Although Trp residue can confer potent antimicrobial activity against AMPs, multiple Trp residues can cause severe hemolytic activity and cytotoxicity.

In this study, to obtain selective short AMPs without hemolytic activity, BP100-W was designed by replacing Leu-3 at the hydrophobic face of BP100 with Trp. The key physicochemical parameters of BP100 and BP100-W are presented in Table 1. The purities of synthetic BP100 and

Table 1 Amino acid sequences and physicochemical properties of BP100 and BP100-W

Peptides	Amino acid sequence	Molecular mass (Da)		Net charge	t_R [b]	μH[c]
		Theoretical	Measured[a]			
BP100	KKLFKKILKYL-NH_2	1421.9	1420.74	+5	17.278	0.847
BP100-W	KK**W**FKKILKYL-NH_2	1494.9	1493.79	+5	18.548	0.873

Substituted amino acids are shown in bold and underlined

[a] Molecular mass was determined using matrix-assisted laser desorption/ionization (MALDI)-time-of-flight (TOF)-mass spectrometry (MS)

[b] Retention time (t_R) was measured using a C-18 reverse phase analytical high-performance liquid chromatography (HPLC) column (5 mm; 4.6 mm × 250 mm; Vydac). The peptides were eluted for 60 min using a linear gradient of 0 – 90% (v/v) acetonitrile in water containing 0.05% (v/v) trifluoroacetic acid (TFA)

[c] Hydrophobicity moment (μH) was calculated online at: http://heliquest.ipmc.cnrs.fr/cgi-bin/ComputParams.py

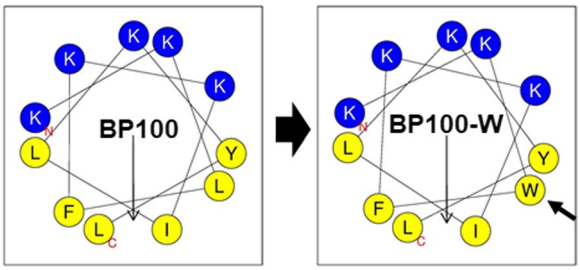

Fig. 1 Helical wheel projection diagrams of BP100 and BP100-W. Positively charged residues (polar) are represented by blue circles and hydrophobic (nonpolar) residues are represented by yellow circles

BP100-W were confirmed to be ≥ 95% using analytical reverse phase high-performance liquid chromatography (RP-HPLC) (Fig. 2a). The theoretical molecular weight of each peptide was confirmed using MALDI-TOF MS spectrometry (Fig. 2b; Table 1). The calculated and measured molecular weights of the peptides were consistent, confirming that BP100 and BP100-W were accurately synthesized. HPLC retention time is an important indicator of the relative hydrophobicity of peptides. HPLC retention times of BP100 and BP100-W were 17.287 and 18.548 min, respectively (Fig. 2a), indicating that BP100-W is slightly more hydrophobic than BP100.

CD spectroscopy

To further examine the secondary structure of the peptides in different environments, CD spectra were measured in an aqueous environment (10 mM PBS) and in bacterial membrane mimicking environments (50% TFE and 30 mM SDS micelles). As shown in Fig. 3, BP100 and BP100-W had negative peaks at 208 and 222 nm, respectively, and a positive peak at 192 nm, characteristic of an α-helical structure, indicating that they have a stable α-helical conformation. However, the spectra of BP100 and BP100-W in 10 mM PBS are characteristic of unordered conformations. In the presence of 50% TFE, BP100 showed a slightly higher helical content than BP100-W, whereas the two peptides displayed a similar helical content in the presence of 30 mM SDS.

Antimicrobial activity and cell selectivity

Minimum inhibitory concentration (MIC) was determined to evaluate the antimicrobial activities of BP100 and BP100-W against six standard bacteria and four antibiotic-resistant bacteria. MICs and geometric means (GMs) of BP100 and BP100-W are listed in Table 2. GM value of BP100 and BP100-W was 16.8 and 10.0 μM, respectively. BP100-W showed a slightly higher antimicrobial activity than BP100. To determine the efficacy of the peptides as antimicrobial drugs, the therapeutic index (TI) was calculated from the ratio of minimal hemolytic concentration (MHC) and the GM for the tested bacteria. MHC is the concentration that causes 10% hemolysis of sRBCs. TI is a widely accepted parameter to evaluate the cell selectivity of antimicrobial agents against bacteria and mammalian cells. As shown in Table 2, BP100-W exhibited better cell selectivity, with a 1.7-fold TI value compared to that of BP100.

Synergistic activity with conventional antibiotics

Combining AMPs with conventional antibiotics has proved to be a successful strategy for combating drug resistance and increasing the antimicrobial activity (Kumar and Shin 2020; Yasir et al. 2020). However, the exact mechanism of action responsible for the synergistic effects in the combination of AMPs and antibiotics remains unclear. We investigated the synergistic activity of BP100 and BP100-W in combination with conventional antibiotics using a checkerboard titration assay. Conventional antibiotics were selected based on their ability to target different bacterial mechanisms, such as protein synthesis (CHL), DNA synthesis (CIP) and cell wall biosynthesis (OXA). The calculated fractional inhibitory concentration index (FICI) values of the peptide-antibiotic combinations against MDRPA and MRSA are listed in Tables 3 and 4. BP100-W showed synergistic antimicrobial activity in combination with CHL, CIP and

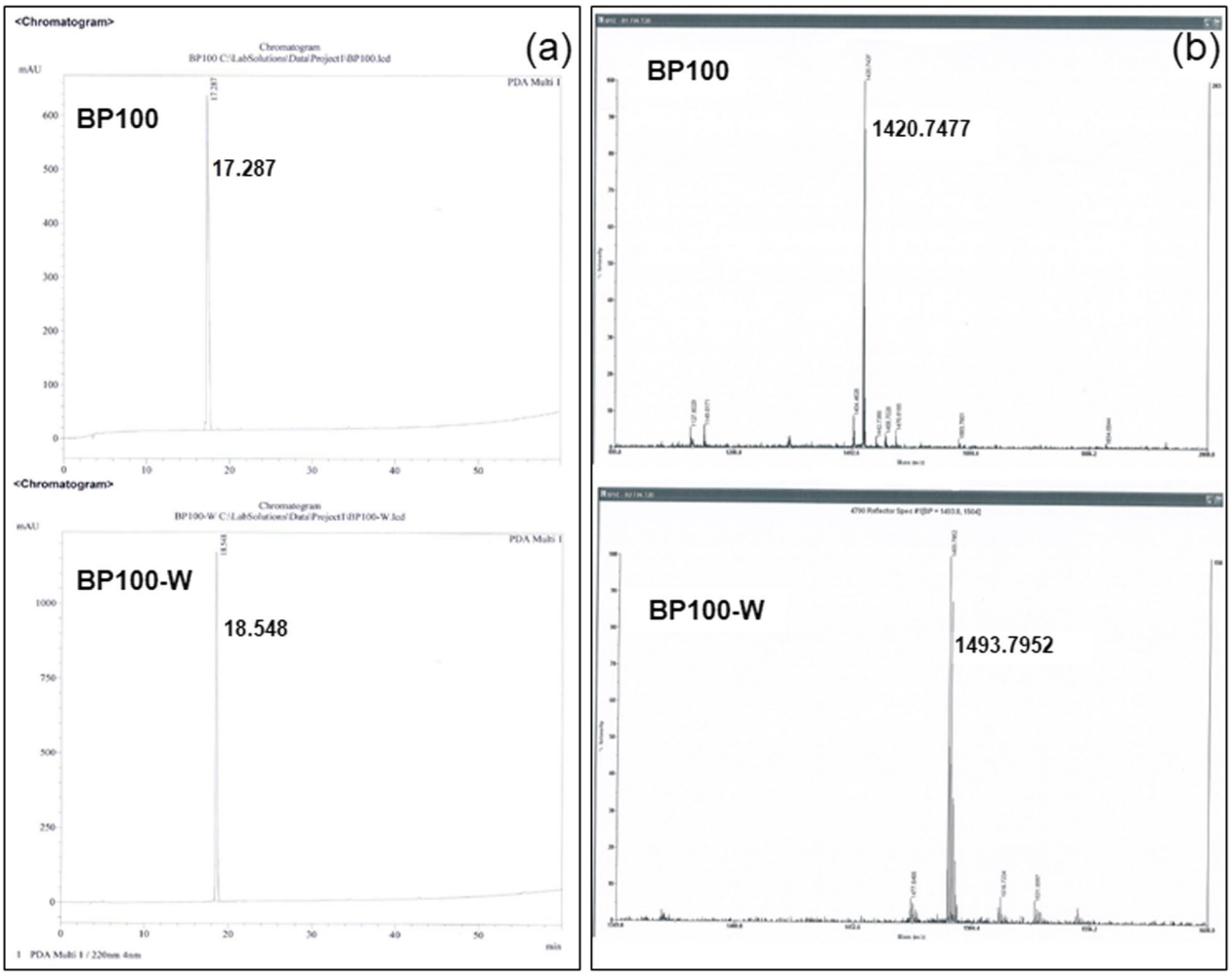

Fig. 2 **a** Reverse phase high-performance liquid chromatography (RP-HPLC) analysis of BP100 and BP100-W. **b** Matrix-assisted laser desorption/ionization-time-of-flight-mass spectrometry (MALDI-TOF–MS) for BP100 and BP100-W

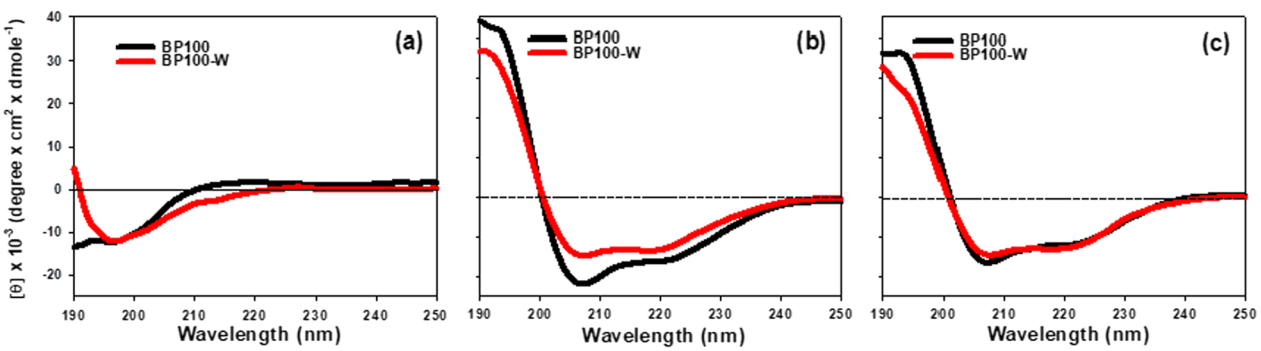

Fig. 3 Circular dichroism (CD) spectra of BP100 and BP100-W in the presence of 10 mM sodium phosphate buffer (pH 7.4) (**a**), 50% TFE (**b**), and 30 mM sodium dodecyl sulfate (SDS) (**c**)

Table 2 Antimicrobial and hemolytic activities and therapeutic index (TI) of BP100 and BP100-W

Bacterial strains	MIC[a] (μM)	
	BP100	BP100-W
Gram-negative bacteria		
Escherichia coli (KCTC 1682)	4	2
Pseudomonas aeruginosa (KCTC 1637)	16	8
Salmonella typhimurium (KCTC 1926)	4	4
Gram-positive bacteria		
Bacillus subtilis (KCTC 3068)	8	8
Staphylococcus epidermidis (KCTC 1917)	4	2
Staphylococcus aureus (KCTC1621)	4	4
Multidrug-resistant *P. aeruginosa (MDRPA)*		
MDRPA 1 (CCARM 2095)	16	8
MDRPA 2 (CCARM 2109)	16	16
Multidrug-resistant *S. aureus (MRSA)*		
MRSA 1 (CCARM 3089)	32	16
MRSA 2 (CCARM 3090)	64	32
GM (μM)[b]	16.8	10.0
MHC (μM)[c]	512 <	512 <
TI (MHC/GM)[d]	60.9	102.4

[a] Minimum inhibitory concentration (MIC) was determined as the lowest concentration of the peptide that inhibited bacterial growth

[b] Geometric mean (GM) denotes the geometric mean of MIC values from the selected bacterial strains

[c] Minimal hemolytic concentration (MHC) is the peptide concentration that causes 10% hemolysis of sheep red blood cells (sRBCs)

[d] Therapeutic index (TI) is the ratio of MHC value (μM) to GM (μM)

OXA against MDRPA, and with CHL and OXA against MRSA. BP100 exhibited synergistic activity in combination with CHL and CIP against MDRPA, and with OXA against MRSA. Overall, BP100-W displayed more effective synergistic activity in combination with conventional antibiotics than BP100. These results demonstrate that BP100 and BP100-W is a broad-spectrum antimicrobial drug effective against multidrug-resistant bacteria and that some antibiotic-resistant bacteria can potentially be eradicated by combining clinically used antibiotics with BP100 and BP100-W.

Antibiofilm activity

Biofilms are bacterial communities enclosed by a self-produced exopolysaccharide matrix (EPM). EPM tends to protect the bacteria from antibiotics. Once biofilms are formed, they can develop up to 10–1000 times more antibiotic resistance than their planktonic counterparts (Jefferson 2004). Bacterial biofilm formation aids in disease pathogenicity and drug resistance development. Therefore, there is an urgent need to develop antimicrobial agents that can neutralize antibiotic resistance and possess potent antibiofilm activity. Although AMPs possess potent antimicrobial activity, only a few of them are able to inhibit biofilm formation and eradicate established bacterial biofilms. As MDRPA is a major cause of hospital-acquired infection through biofilm formation, we explored the effects of BP100 and BP100-W on biofilm formation and eradication of MDRPA using MBIC and MBEC. Here, a human-derived AMP, cathelicidin LL-37, which shows potent antibiofilm activity, was used as a positive control antibiofilm AMP. As shown in Fig. 4, BP100 and BP100-W inhibited biofilm formation by > 90% ($MBIC_{90}$) at 1 × and 2 × MIC, respectively. BP100 and BP100-W showed 50% eradication ($MBEC_{50}$) of mature biofilms at 4 × MIC. In summary, BP100-W was more active than BP100 in inhibiting biofilm formation by MDRPA and eradicating preformed biofilms of MDRPA.

Cytotoxicity on RAW264.7 macrophage cells

Cytotoxic activities of BP100 and BP100-W toward RAW264.7 macrophages were determined using MTT assay (Fig. 5). RAW264.7 macrophages were treated with

Table 3 Fractional inhibitory concentration index (FICI)[a] of peptides in combination with conventional antibiotics against multidrug-resistant *Pseudomonas aeruginosa* (MDRPA) (CCARM 2095)

Combinations		MIC_A (μM)	[A] (μM)	FIC_A	MIC_B (μM)	[B] (μM)	FIC_B	FICI	Combination effect
A: Antibiotics	B: Peptides								
Chloramphenicol	BP100	1024	128	0.125	16	4	0.25	0.375	Synergy
Chloramphenicol	BP100-W	1024	256	0.25	16	4	0.25	0.5	Synergy
Ciprofloxacin	BP100	1024	128	0.125	16	4	0.25	0.375	Synergy
Ciprofloxacin	BP100-W	1024	64	0.0625	16	4	0.25	0.3125	Synergy
Oxacillin	BP100	1024	256	0.25	16	8	0.5	0.75	Additive
Oxacillin	BP100-W	1024	128	0.125	16	4	0.25	0.375	Synergy

MIC_A: MIC of antibiotic A alone, [A]: MIC of antibiotic A in combination. $FIC_A = [A]/MIC_A$

MIC_B: MIC of peptide B alone, [B]: MIC of peptide B in combination. $FIC_B = [B]/MIC_B$

[a] $FICI = FIC_A + FIC_B$. $FICI \leq 0.5$ is synergy, $0.5 < FICI \leq 1.0$ is additive, $1.0 < FICI \leq 4.0$ is indifferent

Table 4 FICI[a] of the peptides in combination with conventional antibiotics against methicillin-resistant *Staphylococcus aureus* (MRSA) (CCARM 3089)

Combinations		MIC_A (μM)	[A] (μM)	FIC_A	MIC_B (μM)	[B] (μM)	FIC_B	FICI	Combination effect
A: Antibiotics	B: Peptides								
Chloramphenicol	BP100	1024	256	0.25	32	16	0.5	0.75	Additive
Chloramphenicol	BP100-W	1024	128	0.125	32	4	0.125	0.25	Synergy
Ciprofloxacin	BP100	1024	1024	1	32	0.5	0.0156	1.0156	Indifferent
Ciprofloxacin	BP100-W	1024	1	0.001	32	16	0.5	0.501	Indifferent
Oxacillin	BP100	1024	128	0.125	32	8	0.25	0.375	Synergy
Oxacillin	BP100-W	1024	64	0.0625	32	8	0.25	0.3125	Synergy

MIC_A: MIC of antibiotic A alone, [A]: MIC of antibiotic A in combination. $FIC_A = [A]/MIC_A$

MIC_B: MIC of peptide B alone, [B]: MIC of peptide B in combination. $FIC_B = [B]/MIC_B$

[a] $FICI = FIC_A + FIC_B$. $FICI \leq 0.5$ is synergy, $0.5 < FICI \leq 1.0$ is additive, $1.0 < FICI \leq 4.0$ is indifferent

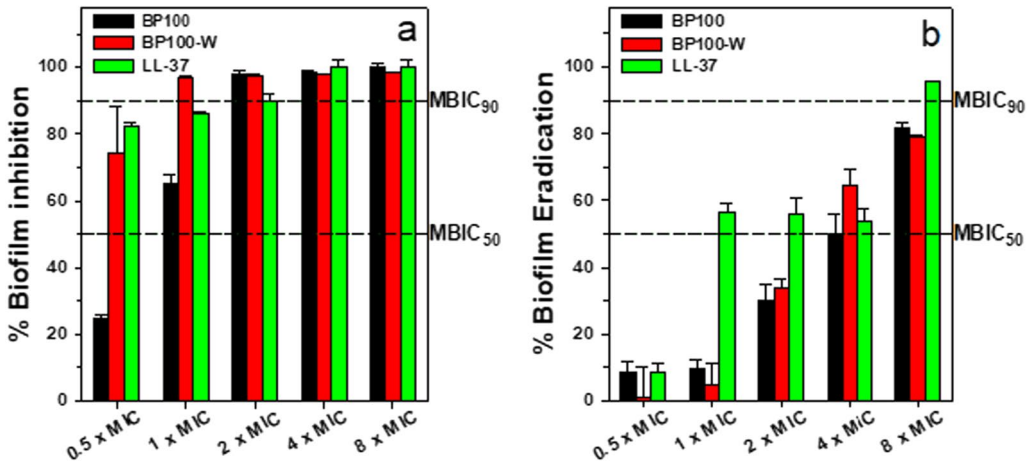

Fig. 4 In vitro antibiofilm activities of BP100, BP100-W and LL-37 against multidrug-resistant *Pseudomonas aeruginosa* (MDRPA). **a** Biofilm inhibition. **b** Biofilm eradication. Dashed lines indicate 50 and 90% inhibition and eradication concentration

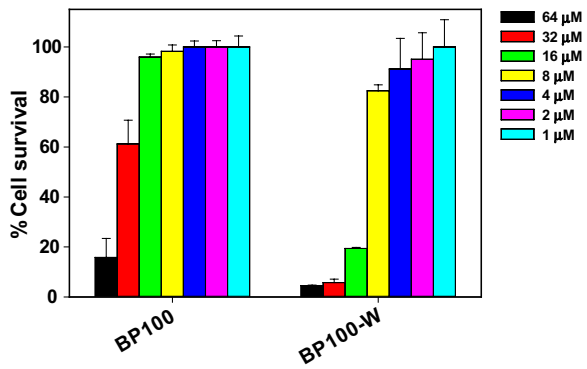

Fig. 5 Cytotoxicities of BP100 and BP100-W against RAW264.7 mouse macrophages

peptides at various concentrations ranging from 1 to 64 μM. These data indicate both BP100 and BP100-W were minimally cytotoxic at 8 μM and thus suitable for further anti-inflammatory experiments.

Anti-inflammatory activity

LPS is the major cell wall component of gram-negative bacteria and can induce severe endotoxemia at high concentrations in the blood (Rosenfeld et al. 2006; Trent et al. 2006). LPS is the prototype stimulator that triggers an inflammatory cascade in macrophages via the Toll-like receptor 4 (TLR4) (Oberholzer et al. 2001). NO and TNF-α, which are representative inflammation-inducing factors, play critical roles in the development

of innate immunity during septic shock, and inflammation induced by LPS (Kim et al. 2017). To evaluate the anti-inflammatory activities of BP100 and BP100-W, their effects on the production and expression of representative pro-inflammatory cytokines, NO and TNF-α, in LPS-stimulated RAW 264.7 cells were determined by sandwich ELISA and RT-PCR. NO production was determined by the Griess method, which detects nitrite ion (NO_2^-) accumulation in the culture medium (Fig. 6a). Inhibitory effect of the peptides on the release of TNF-α in LPS-stimulated RAW264.7 cells was investigated using commercially available ELISA kits (Fig. 6b). BP100-W was more effective in inhibiting NO and TNF-α production than BP100. Similar to LL-37 (a powerful anti-inflammatory AMP), BP100-W inhibited the production of NO and TNF-α in LPS-stimulated RAW264.7 cells at a concentration of 8 μM with a similar activity as that of LL37, a potent anti-inflammatory AMP (Fig. 6). The mRNA expression levels of inducible nitric oxide synthase (iNOS) and TNF-α were determined using RT-PCR (Fig. 6c). BP100-W was as effective as LL-37 in suppressing iNOS and TNF-α expression. These data were in good agreement with the observed inhibition of the NO and TNF-α release by the peptides. These results suggest that BP100-W has the potential to be developed as an anti-inflammatory agent that blocks LPS-mediated inflammatory mediators.

Most AMPs exert their anti-inflammatory effect by direct binding to extracellular LPS (Kim et al. 2017; Rosenfeld et al. 2006; Scott et al. 2011). Therefore, to investigate whether these peptides inhibited LPS-induced inflammation through direct binding to LPS, we performed the boron-dipyrromethene-TR-cadaverine (BC) displacement assay. Initially, BC fluorescence was quenched when bound to free LPS. The introduction of antiendotoxin compounds displaces BC, its fluorescence increased, indicating the successful binding

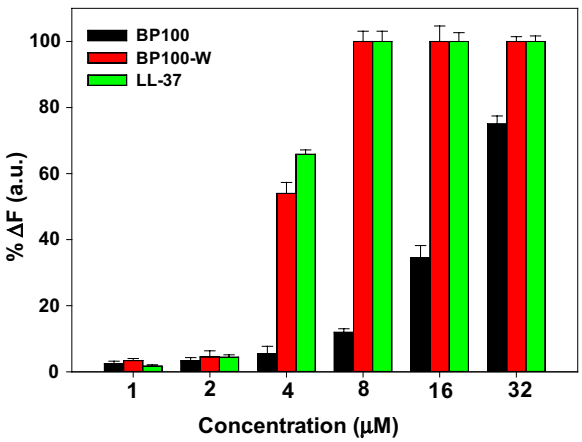

Fig. 7 Binding abilities of BP100, BP100-W and LL-37 to LPS from *Escherichia coli* 0111:B4 using boron-dipyrromethene (BODIPY)-TR-cadaverine displacement. Fluorescence intensity was monitored at an excitation wavelength of 580 nm and emission wavelength of 620 nm

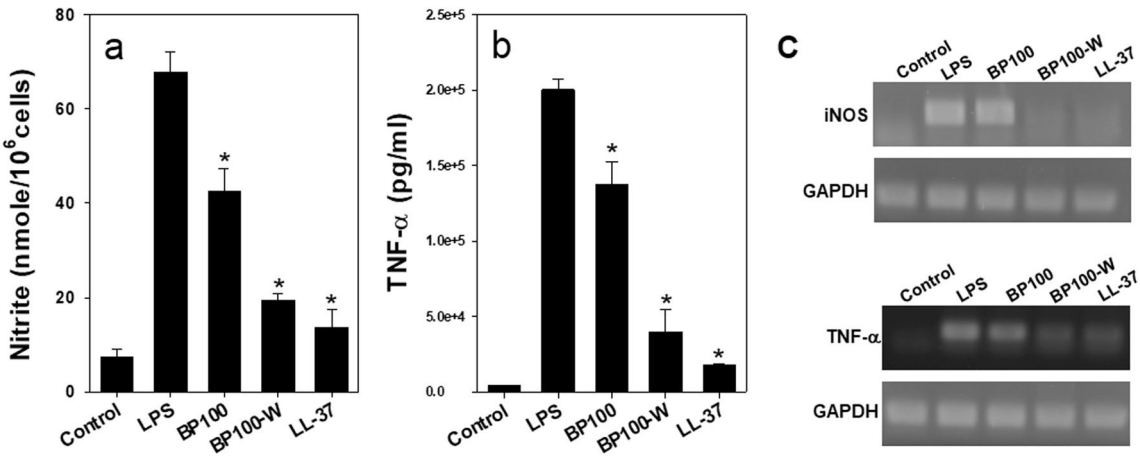

Fig. 6 **a** Effects of BP100 and BP100-W on nitric oxide (NO) production in lipopolysaccharide (LPS)-stimulated RAW264.7 cells. **b** Effects of BP100 and BP100-W on tumor necrosis factor (TNF)-α release from LPS-stimulated RAW264.7 cells. Concentration of peptides used for this experiment is 8 μM. All data represent at least three independent experiments and are expressed as the mean ± standard error of the mean (SEM). Data were analyzed using one-way analysis of variance (ANOVA) with Bonferroni's post-test. Asterisks indicate the statistically significant differences (*$P < 0.001$ for each agonist). **c** Effects of BP100 and BP100-W on the mRNA levels of inducible nitric oxide synthase (iNOS) and TNF-α in LPS-stimulated RAW264.7 cells. RAW264.7 cells (5×10^5 cells/well) were incubated with the peptides in the presence of LPS (20 ng/mL) for 3 h (for TNF-α) or 6 h (for iNOS). Total RNA was isolated and analyzed to determine the mRNA levels of iNOS and TNF-α using reverse transcription-polymerase chain reaction (RT-PCR). Concentration of peptides used for this experiment is 8 μM

of the compound with LPS. As shown in Fig. 7, BP100-W showed more than 50% and 100% binding ability to LPS at 4 μM and 8 μM, respectively, similar to LL-37, a potent LPS-binding AMP. In contrast, BP100 displayed a poor LPS-binding ability of less than 20% at 8 μM and did not reach 100% LPS-binding ability even at a high concentration of 32 μM. These results suggested that the inhibitory activity of BP100-W on LPS-induced inflammation in RAW 264.7 cells may be due to its increased direct interaction with LPS.

Conclusions

In summary, we developed a novel short AMP, BP100-W, with antimicrobial, antibiofilm and anti-inflammatory activities by replacing Leu-3 at the hydrophobic face of BP100 with Trp. BP100-W showed better selectivity for bacterial cells, with a 1.7-fold TI compared to that of BP100. BP100-W showed more effective synergistic activity in combination with conventional antibiotics, such as CHL, CIP and OXA than BP100. BP100-W possessed stronger antibiofilm activity than BP100 in inhibiting biofilm formation by MDRPA and eradicating the preformed biofilms of MDRPA. Furthermore, unlike BP100, BP100-W significantly inhibited the expression and production of pro-inflammatory cytokines, such as NO and TNF-α, in LPS-stimulated RAW264.7 cells. Furthermore, the inhibitory activity of BP100-W on LPS-induced inflammation in RAW 264.7 cells may be due to its increased direct interaction with LPS. Our results indicate that BP100-W shows considerable potential for future use as an antimicrobial, antibiofilm and anti-inflammatory agent.

Abbreviations

AMP: Antimicrobial peptide; CD: Circular dichroism; GM: Geometric mean; LPS: Lipopolysaccharide; MBIC: Minimum biofilm inhibitory concentration; MBEC: Minimum biofilm eradication concentration; MDRPA: Multidrug-resistant *Pseudomonas aeruginosa*; MHC: Minimal hemolytic concentration; MIC: Minimum inhibitory concentration; MRSA: Methicillin-resistant *Staphylococcus aureus*; sRBCs: Sheep red blood cells; TFA: Trifluoroacetic acid; TI: Therapeutic index; TNF-α: Tumor necrosis factor-α.

Acknowledgements

Not applicable.

Author contributions

SYS designed the study. CA, SDK, EYK and SY performed the experiments. SYS and CA interpreted the data and drafted the manuscript. All authors read and approved the final manuscript.

Funding

This work was supported by the research fund from Chosun University, 2022.

Availability of data and materials

Not applicable.

Declarations

Competing interests

The authors declare that they have no competing interests.

Author details

[1]Department of Cellular and Molecular Medicine, School of Medicine, Chosun University, Gwangju 61452, Republic of Korea. [2]Department of Microbiology, School of Medicine, Chosun University, Gwangju 61452, Republic of Korea.

Received: 26 October 2022 Accepted: 24 November 2022
Published online: 14 December 2022

References

Arias M, Nguyen LT, Kuczynski AM, Lejon T, Vogel HJ. Position-dependent influence of the three Trp residues on the membrane activity of the antimicrobial peptide, tritrpticin. Antibiotics (basel). 2014;3:595–616. https://doi.org/10.3390/antibiotics3040595.

Badosa E, Ferre R, Planas M, Feliu L, Besalu E, Cabrefiga J, Bardaji E, Montesinos E. A library of linear undecapeptides with bactericidal activity against phytopathogenic bacteria. Peptides. 2007;28:2276–85. https://doi.org/10.1016/j.peptides.

Basak A, Abouelhassan Y, Zuo R, Yousaf H, Ding Y, Huigens RW. Antimicrobial peptide-inspired NH125 analogues: bacterial and fungal biofilm-eradicating agents and rapid killers of MRSA persisters. Org Biomol Chem. 2017;15:5503–12. https://doi.org/10.1039/c7ob01028a.

Bastos M, Bai G, Gomes P, Andreu D, Goormaghtigh E, Prieto M. Energetics and partition of two cecropin-melittin hybrid peptides to model membranes of different composition. Biophys J. 2008. https://doi.org/10.1529/biophysj.107.119032.

Bi X, Wang C, Dong W, Zhu W, Shang D. Antimicrobial properties and interaction of two Trp-substituted cationic antimicrobial peptides with a lipid bilayer. J Antibiot. 2014;67:361–8. https://doi.org/10.1038/ja.2014.4.

Dong N, Ma Q, Shan A, Lv Y, Hu W, Gu Y, Li Y. Strand length-dependent antimicrobial activity and membrane-active mechanism of arginine- and valine-rich beta-hairpin-like antimicrobial peptides. Antimicrob Agents Chemother. 2012;56:2994–3003. https://doi.org/10.1128/AAC.06327-11.

Epand RF, Savage PB, Epand RM. Bacterial lipid composition and the antimicrobial efficacy of cationic steroid compounds (Ceragenins). Biochim Biophy Acta. 2007;1768:2500–9. https://doi.org/10.1016/j.bbamem.2007.05.023.

Ferre R, Melo MN, Correia AD, Feliu L, Bardaji E, Planas MJ, Castanho M. Synergistic effects of the membrane actions of cecropin-melittin antimicrobial hybrid peptide BP100. Biophys J. 2009;96:1815–27. https://doi.org/10.1016/j.bpj.2008.11.053.

Ghosh A, Kar RK, Jana J, Saha A, Jana B, Krishnamoorthy J, Kumar D, Ghosh S, Chatterjee S, Bhunia A. Indolicidin targets duplex DNA: structural and mechanistic insight through a combination of spectroscopy and microscopy. ChemMedChem. 2014;9:2052–8. https://doi.org/10.1002/cmdc.201402215.

Harrison JJ, Stremick CA, Turner RJ, Allan ND, Olson ME, Ceri H. Microtiter susceptibility testing of microbes growing on peg lids: a miniaturized biofilm model for high throughput screening. Nat Protoc. 2010;5:1236–54. https://doi.org/10.1038/nprot.2010.71.

Hilpert K, McLeod B, Yu J, Elliott MR, Rautenbach M, Ruden S, Bürck J, Muhle-Goll C, Ulrich AS, Keller S, Hancock RE. Short cationic antimicrobial peptides interact with ATP. Antimicrob Agents Chemother. 2010;54:4480–3. https://doi.org/10.1128/AAC.01664-09.

Hsu CH, Chen C, Jou ML, Lee AY, Lin YC, Yu YP, Huang WT, Wu SH. Structural and DNA-binding studies on bovine antimicrobial peptide, indolicidin: evidence for multiple conformations involved in binding to membranes and DNA. Nucleic Acids Res. 2005;33:4053–64. https://doi.org/10.1093/nar/gki725.

Jefferson KK. What drives bacteria to produce a biofilm? FEMS Microbiol Lett. 2004;236:163–73. https://doi.org/10.1016/j.femsle.2004.06.005.

Juvvadi P, Vunnam S, Merrifield EL, Boman HG, Merrifield RB. Hydrophobic effects on antibacterial and channel-forming properties of cecropin A-melittin hybrids. J Pept Sci. 1996;2:223–32. https://doi.org/10.1002/psc.63.

Khara JS, Wang Y, Ke XY, Liu S, Newton SM, Langford PR, Yang YY, Ee PLR. Anti-mycobacterial activities of synthetic cationic α-helical peptides and their synergism with rifampicin. Biomaterials. 2014;35:2032–8. https://doi.org/10.1016/j.biomaterials.2013.11.035.

Killian JA, von Heijne G. How proteins adapt to a membrane-water interface. Trends Biochem Sci. 2000;25:429–34. https://doi.org/10.1016/s0968-0004(00)01626-1.

Kim EY, Rajasekaran G. Shin SY, LL-37-derived short antimicrobial peptide KR-12-a5 and its d-amino acid substituted analogs with cell selectivity, anti-biofilm activity, synergistic effect with conventional antibiotics, and anti-inflammatory activity. Eur J Med Chem. 2017;136:428–41. https://doi.org/10.1016/j.ejmech.2017.05.028.

Kumar SD, Shin SY. Antimicrobial and anti-inflammatory activities of short dodecapeptides derived from duck cathelicidin: plausible mechanism of bactericidal action and endotoxin neutralization. Eur J Med Chem. 2020;204: 112580. https://doi.org/10.1016/j.ejmech.2020.112580.

Marchand C, Krajewski K, Lee HF, Antony S, Johnson AA, Amin R, Roller P, Kvaratskhelia M, Pommier Y. Covalent binding of natural antimicrobial peptide indolicidin to DNA abasic sites. Nucleic Acids Res. 2006;34:5157–65. https://doi.org/10.1093/nar/gkl667.

Mishra AK, Choi J, Moon E, Baek KH. Tryptophan-rich and proline-rich antimicrobial peptides. Molecules. 2018;23:815. https://doi.org/10.3390/molecules23040815.

Oberholzer A, Oberholzer C, Moldawer LL. Sepsis syndromes: understanding the role of innate and acquired immunity. Shock. 2001;16:83–96. https://doi.org/10.1097/00024382-200116020-00001.

Rajasekaran G, Kumar SD, Yang S, Shin SY. The design of a cell-selective fowlicidin-1-derived peptide with both antimicrobial and anti-inflammatory activities. Eur J Med Chem. 2019;182:111623. https://doi.org/10.1016/j.ejmech.2019.111623.

Rosenfeld Y, Papo N, Shai Y. Endotoxin (lipopolysaccharide) neutralization by innate immunity host-defense peptides. J Biol Chem. 2006;281:1636–43. https://doi.org/10.1074/jbc.M504327200.

Sanchez KM, Kang G, Wu B, Kim JE. Tryptophan-lipid interactions in membrane protein folding probed by ultraviolet resonance Raman and fluorescence spectroscopy. Biophys J. 2011;100:2121–30. https://doi.org/10.1016/j.bpj.2011.03.018.

Scott A, Weldon S, Buchanan PJ, Schock B, Ernst RK, McAuley DF, Tunney MM, Irwin CR, Elborn JS, Taggart CC. Evaluation of the ability of LL-37 to neutralise LPS in vitro and ex vivo. PLoS ONE. 2011;6:e26525. https://doi.org/10.1371/journal.pone.0026525.

Sharma R, Lomash S, Salunke DM. Putative bioactive motif of tritrpticin revealed by an antibody with biological receptor-like properties. PLoS ONE. 2013;8:e75582. https://doi.org/10.1371/journal.pone.0075582.

Sitaram N, Subbalakshmi C, Nagaraj R. Indolicidin, a 13-residue basic antimicrobial peptide rich in tryptophan and proline, interacts with calcium(2+)-calmodulin. Biochem Biophys Res Commun. 2003;309:879–84. https://doi.org/10.1016/j.bbrc.2003.08.095.

Torcato IM, Huang YH, Franquelim HG, Gaspar D, Craik DJ, Castanho MA, Henriques ST. Design and characterization of novel antimicrobial peptides, R-BP100 and RW-BP100, with activity against Gram-negative and Gram-positive bacteria. Biochim Biophys Acta. 2013;1828:944–55. https://doi.org/10.1016/j.bbamem.2012.12.002.

Trent MS, Stead MC, Tran AX, Hankins JV. Diversity of endotoxin and its impact on pathogenesis. J Endotoxin Res. 2006;12:205–23. https://doi.org/10.1179/096805106X118825.

Wei SY, Wu JM, Kuo YY, Chen HL, Yip BS, Tzeng SR, Cheng JW. Solution structure of a novel tryptophan-rich peptide with bidirectional antimicrobial activity. J Bacteriol. 2006;188:328–34. https://doi.org/10.1128/JB.188.1.328-334.2006.

Wiegand I, Hilpert K, Hancock RE. Agar and broth dilution methods to determine the minimal inhibitory concentration (MIC) of antimicrobial substances. Nat Protoc. 2008;3:163–75. https://doi.org/10.1038/nprot.2007.521.

Wood SJ, Miller KA, David SA. Anti-endotoxin agents. 1. Development of a fluorescent probe displacement method optimized for the rapid identification of lipopolysaccharide-binding agents. Comb Chem High Throughput Screen. 2004;7:239–49. https://doi.org/10.2174/1386207043328832.

Yasir M, Dutta D, Willcox MDP. Activity of antimicrobial peptides and ciprofloxacin against *Pseudomonas aeruginosa* biofilms. Molecules. 2020;25:3843. https://doi.org/10.3390/molecules25173843.

Yau WM, Wimley WC, Gawrisch K, White SH. The preference of tryptophan for membrane interfaces. Biochemistry. 1998;37:14713–8. https://doi.org/10.1021/bi980809c.

Zhu X, Dong N, Wang Z, Ma Z, Zhang L, Ma Q, Shan A. Design of imperfectly amphipathic α-helical antimicrobial peptides with enhanced cell selectivity. Acta Biomater. 2014;10:244–57. https://doi.org/10.1016/j.actbio.2013.08.043.

Publisher's Note